J. Dairy Sci. 108:8637–8647
https://doi.org/10.3168/jds.2025-26361

Bayesian fine-mapping and Mendelian randomization leveraging expression quantitative trait loci reveal novel candidate causal genes for body conformation traits in cattle

Jun Teng,[1] Chongwei Duan,[1] Xinyi Zhang,[1] Zhujun Chen,[1] Chao Ning,[1] Rongling Li,[2] Yundong Gao,[2] Hongding Gao,[3] Huiming Liu,[4] Jianbin Li,[2] Xiao Wang,[2]* and Qin Zhang[1]*

[1]Shandong Provincial Key Laboratory for Livestock Germplasm Innovation and Utilization, College of Animal Science and Technology, Shandong Agricultural University, Tai'an 271018, Shandong, China
[2]Institute of Animal Science and Veterinary Medicine, Shandong Academy of Agricultural Sciences, Jinan 250100, China
[3]Natural Resources Institute Finland (Luke), Jokioinen 31600, Finland
[4]Center for Quantitative Genetics and Genomics, Aarhus University, Aarhus 8000, Denmark

ABSTRACT

Cattle body size measurements constitute the conformation traits that facilitate their production, fertility, and longevity status. Prioritizing functional variants and causal genes of conformation traits is essential for understanding their genetic basis. In this study, we conducted single-trait and multitrait GWAS for 20 body conformation traits using imputed sequence data in 7,674 Chinese Holstein individuals and identified 27 QTL regions. Leveraging these QTL regions, we performed multitrait Bayesian fine-mapping to identify 30 independent credible sets of putative causal variants. Incorporating GWAS and *cis*-acting expression QTL data, Mendelian randomization was used to infer 153 putative causal gene-trait relationships. The previously reported genes, such as *CCND2*, *TMTC2*, and *NRG3*, were confirmed in our study. Of note, several novel candidate causal genes were also identified, such as *C1R*, *RIMS1*, *SERPINB8*, *NETO2*, *TTYH3*, *TTC3*, *ANAPC4*, and *PSMD13*. Our results provide new insights into the regulatory mechanisms of body conformation traits in cattle.
Key words: GWAS, Bayesian fine-mapping, Mendelian randomization, body conformation traits, cattle

INTRODUCTION

With the 1000 Bull Genomes Project and rapid reduction of sequencing costs (Hayes and Daetwyler, 2019), an increasing number of GWAS leveraging sequence-level data have deciphered the genetic architecture of cattle complex traits (Jiang et al., 2019a; Pedrosa et al., 2021). However, the high-level linkage disequilibrium (**LD**) in cattle populations (Kim and Kirkpatrick, 2009) complicates the identification of causal trait-associated variants. Several Bayesian methods for fine-mapping to single-variant resolution, such as BIMBAM (Servin and Stephens, 2007), FINEMAP (Benner et al., 2016), and SuSiE (Wang et al., 2020), have been developed to prioritize putative causal variants underlying complex traits in humans (Singh et al., 2023; Hemerich et al., 2024).

The circumstances of most GWAS signals residing in noncoding regions imply the regulatory roles of genetic variants for gene regulation through underlying mechanisms (Uffelmann et al., 2021; Qi et al., 2024). Many identified *cis*- or *trans*-acting expression QTL (eQTL) combining GWAS signals could be a robust way to infer causal trait-associated genes (Mai et al., 2023) using transcriptome-wide association studies (Gusev et al., 2016) or Mendelian randomization (**MR**; Qi et al., 2024) approaches. Mendelian randomization analysis aims to determine the causal gene-trait relationship between an exposure variable (e.g., gene expression) and an outcome variable (e.g., trait) regarding SNPs as instrumental variables (Yang et al., 2021; Chepelev et al., 2023; Jiang et al., 2023) based on MR-Egger (Bowden et al., 2015), summary data–based MR (Zhu et al., 2016), and probabilistic MR-Egger (**PMR-Egger**; Yuan et al., 2020) methods.

Breeding objectives for dairy cattle are multifaceted and encompass milk production, health, body conformation, fertility, and longevity traits. Among these traits, body conformation traits, which are closely related to milk production performance, health, and longevity, are essential components for evaluating the total performance index of dairy cattle (Köck et al., 2018; Wang et al., 2024). Many genetic variants associated with body

Received January 22, 2025.
Accepted April 24, 2025.
*Corresponding authors: xiaowangzntc@163.com and qzhang@sdau.edu.cn

The list of standard abbreviations for JDS is available at adsa.org/jds-abbreviations-25. Nonstandard abbreviations are available in the Notes.

conformation traits in dairy cattle have been identified (Wu et al., 2013; Haque et al., 2023; Li et al., 2024), but the identification of causal variants and their regulatory roles have rarely been reported. Therefore, this study aims to identify causal variants for body conformation traits in fine-mapping regions from GWAS using the imputed sequence genotypes in a Chinese Holstein population. Furthermore, GWAS and eQTL summary data were leveraged to identify causal genes. Our results provided novel insights into the identification of putative functional genes and enhance our understanding of regulatory mechanisms of body conformation traits in dairy cattle.

MATERIALS AND METHODS

Phenotypes and Genotypes

In this study, we used a Chinese Holstein population containing 7,674 cows with 5 groups of body conformation traits, including body, rump, feet and legs, mammary system, and dairy character. The traits are as follows: (1) body traits: body height (**BH**), chest width (**CW**), body depth (**BD**) and loin strength (**LS**); (2) rump traits: pin setting (**PS**) and thurl width (**TW**); (3) feet and legs traits: foot angle (**FAN**), heel depth (**HD**), bone quality (**BQ**), rear legs side view (**RLSV**) and rear legs rear view (**RLRV**); (4) mammary system traits: udder depth (**UD**), median suspensory (**MSP**), fore attachment (**FAC**), fore teat placement (**FTP**), teat length (**TL**), rear attach height (**RAH**), rear attach width (**RAW**) and rear teat placement (**RTP**); and (5) dairy character trait: angularity (**ANG**). All 20 traits were scored on a scale from 1 to 9 as the linear descriptive traits (Supplemental Table S1, see Notes).

These cows were genotyped using SNP chips with different densities (50K, 100K, and 150K). Then, as the reference panel, we used the sequencing data of 3,530 cattle (average sequencing depth greater than 10×) obtained from the National Center for Biotechnology Information sequence read archive database (https://www.ncbi.nlm.nih.gov/sra), and imputed the SNP chip genotypes to the whole-genome sequence (**WGS**) level using Beagle v5.1 (Browning et al., 2018) according to our previous study (Teng et al., 2023). To evaluate the imputation accuracy, we sequenced additional 100 cows in our Holstein population with sequencing depth greater than 15×, as validation individuals. Their sequence genotypes were reduced to the corresponding chip genotypes and then imputed to the sequence level. We used r^2 (the squared correlation between the expected dosages and known true genotypes) to measure the imputation accuracy. To reduce computational time, we selected one chromosome (Chr 25) for accuracy assessment. After imputation, SNPs with minor allele frequency (**MAF**) less than 0.05 or with a *P*-value <1 × 10^{-6} for Hardy–Weinberg equilibrium (**HWE**) test were excluded for subsequent analysis.

Heritability and Genetic Correlation Estimation

The following univariate linear mixed model was used to estimate the heritability for each trait:

$$\mathbf{y} = \mathbf{Xb} + \mathbf{Za} + \mathbf{e}, \quad [1]$$

$$\mathbf{a} \sim N\left(0, \mathbf{G}\sigma_a^2\right); \mathbf{e} \sim N\left(0, \mathbf{I}\sigma_e^2\right),$$

where $\mathbf{y}$ is the vector of phenotypic values of the trait; $\mathbf{b}$ is the vector of fixed effects for herd, measurement age, and assessor; $\mathbf{X}$ is the design matrix associating $\mathbf{b}$ with $\mathbf{y}$; $\mathbf{a}$ is the vector of additive genetic effects; $\mathbf{Z}$ is the design matrix associating $\mathbf{a}$ with $\mathbf{y}$; σ_a^2 is the additive genetic variance; $\mathbf{G}$ is the genomic relationship matrix defined by VanRaden (2008); $\mathbf{e}$ is the vector of the random residuals, $\mathbf{I}$ is the identity matrix, N represents the normal distribution, and σ_e^2 is the residual variance. The heritability of the trait was calculated as $h^2 = \frac{\sigma_a^2}{\sigma_a^2 + \sigma_e^2}$. The following bivariate linear mixed model was used to estimate the genetic correlation between 2 traits,

$$\begin{bmatrix}\mathbf{y}_1\\ \mathbf{y}_2\end{bmatrix} = \begin{bmatrix}\mathbf{X}_1 & 0\\ 0 & \mathbf{X}_2\end{bmatrix}\begin{bmatrix}\mathbf{b}_1\\ \mathbf{b}_2\end{bmatrix} + \begin{bmatrix}\mathbf{Z}_1 & 0\\ 0 & \mathbf{Z}_2\end{bmatrix}\begin{bmatrix}\mathbf{a}_1\\ \mathbf{a}_2\end{bmatrix} + \begin{bmatrix}\mathbf{e}_1\\ \mathbf{e}_2\end{bmatrix}, \quad [2]$$

$$\begin{bmatrix}\mathbf{a}_1\\ \mathbf{a}_2\end{bmatrix} \sim \boldsymbol{N}(\mathbf{0}, \mathbf{M} \otimes \mathbf{G}), \begin{bmatrix}\mathbf{e}_1\\ \mathbf{e}_2\end{bmatrix} \sim \boldsymbol{N}(\mathbf{0}, \mathbf{R} \otimes \mathbf{I}),$$

where all terms are the same as those in Model [1], with the subscripts 1 and 2 refering to traits 1 and 2, respectively; $\mathbf{M} = \begin{bmatrix}\sigma_{a_1}^2 & \sigma_{a_{12}}\\ \sigma_{a_{12}} & \sigma_{a_2}^2\end{bmatrix}$, with $\sigma_{a_1}^2$ and $\sigma_{a_2}^2$ being the additive genetic covariance and $\sigma_{a_{12}}$ being the additive genetic variance-covariance for the 2 traits; and $\mathbf{R} = \begin{bmatrix}\sigma_{e_1}^2 & \sigma_{e_{12}}\\ \sigma_{e_{12}} & \sigma_{e_2}^2\end{bmatrix}$, with $\sigma_{e_1}^2$ and $\sigma_{e_2}^2$ being the residual variances and $\sigma_{e_{12}}$ being the residual covariance for the 2 traits. The global genetic correlation was calculated as $r_g = \frac{\sigma_{a_{12}}}{\sqrt{\sigma_{a_1}^2 \sigma_{a_2}^2}}$. The variance and covariance components involved in these 2 models were estimated by residual maximum likelihood algorithm using the GCTA software (Yang et al., 2011).

Genome-Wide Association Studies

Single-trait (**ST**) and multitrait (**MT**) GWAS were performed using GMAT software (Ning et al., 2018) based on the linear mixed model. The following univariate linear mixed model was used to perform ST-GWAS for each trait:

$$\mathbf{y} = \mathbf{Xb} + \mathbf{m}\beta + \mathbf{Za} + \mathbf{e}, \quad [3]$$

$$\mathbf{a} \sim N\left(0, \mathbf{G}\sigma_a^2\right); \mathbf{e} \sim N\left(0, \mathbf{I}\sigma_e^2\right),$$

where **m** is the vector of genotypes of a candidate SNP (coded as 0, 1 or 2) and β is the regression coefficient; the rest of the terms (**y**, **X**, **b**, **Z**, **a**, and **e**) are the same as those in Model [1].

There were 4 trait groups (body, rump, feet and legs, and mammary system) including multiple traits. Thus, we also performed MT-GWAS for traits in each trait group using the following multivariate linear mixed model:

$$\begin{bmatrix}\mathbf{y}_1\\ \mathbf{y}_2\\ \vdots\\ \mathbf{y}_n\end{bmatrix} = \begin{bmatrix}\mathbf{X}_1 & 0 & 0 & 0\\ 0 & \mathbf{X}_2 & 0 & 0\\ 0 & 0 & \ddots & 0\\ 0 & 0 & 0 & \mathbf{X}_n\end{bmatrix}\begin{bmatrix}\mathbf{b}_1\\ \mathbf{b}_2\\ \vdots\\ \mathbf{b}_n\end{bmatrix} + \begin{bmatrix}\mathbf{m}_1 & 0 & 0 & 0\\ 0 & \mathbf{m}_2 & 0 & 0\\ 0 & 0 & \ddots & 0\\ 0 & 0 & 0 & \mathbf{m}_n\end{bmatrix}\begin{bmatrix}\beta_1\\ \beta_2\\ \vdots\\ \beta_n\end{bmatrix} +$$

$$\begin{bmatrix}\mathbf{Z}_1 & 0 & 0 & 0\\ 0 & \mathbf{Z}_2 & 0 & 0\\ 0 & 0 & \ddots & 0\\ 0 & 0 & 0 & \mathbf{Z}_n\end{bmatrix}\begin{bmatrix}\mathbf{a}_1\\ \mathbf{a}_2\\ \vdots\\ \mathbf{a}_n\end{bmatrix} + \begin{bmatrix}\mathbf{e}_1\\ \mathbf{e}_2\\ \vdots\\ \mathbf{e}_n\end{bmatrix} \quad [4]$$

$$\begin{bmatrix}\mathbf{a}_1\\ \mathbf{a}_2\\ \vdots\\ \mathbf{a}_n\end{bmatrix} \sim \boldsymbol{N}\left(0, \boldsymbol{\Sigma}_a \otimes \mathbf{G}\right), \begin{bmatrix}\mathbf{e}_1\\ \mathbf{e}_2\\ \vdots\\ \mathbf{e}_n\end{bmatrix} \sim \boldsymbol{N}\left(0, \boldsymbol{\Sigma}_e \otimes \mathbf{I}\right),$$

where *n* is the *n*th trait in each trait group, and the rest of the terms (**y**, **X**, **b**, **m**, β, **Z**, **a**, and **e**) are the same as those in Models [2] and [3]. The structures of $\boldsymbol{\Sigma}_a$ and $\boldsymbol{\Sigma}_a$ are similar to those in Model [2].

We employed Bonferroni correction to control false-positive rates from multiple testing. The genome-wide significance threshold was set at 0.05/N, where N represents the number of effective SNPs. The effective SNPs were defined as those that were not in high LD. To obtain these SNPs, we performed LD pruning using the PLINK software (Purcell et al., 2007) with the command "–indep-pairwise 50 5 0.2," which defines the window size being 50 SNPs with a step size of 5 SNPs and the LD threshold $\left(r_{LD}^2\right)$ being 0.2.

Multitrait Bayesian Fine-Mapping

To select regions for fine-mapping, we first defined a ST-QTL region for ST-GWAS, which contains a bunch of significant SNPs with distances between adjacent significant SNPs less than 250 kb and bounded by the final significant SNPs at both sides of the bunch. Similarly, we also defined MT-QTL regions for MT-GWAS. Next, for each trait group, we merged ST-QTL regions from different traits and MT-QTL regions whenever they overlapped, and the merged regions were defined as the MT-QTL regions for this trait group. The tested fine-mapping regions were defined as a window covering 250 kb of both sides of those MT-QTL regions. We used the multitrait fine-mapping method, mvSuSiE (Y. Zou, P. Carbonetto, D. Xie, G. Wang, and M. Stephens, University of Chicago, Chicago, IL; unpublished data), to identify putative causal variants within each fine-mapping region in each trait group. mvSuSiE computed cross-trait posterior inclusion probability (**PIP**) for variants within each fine-mapping region, quantifying the evidence that these variants have nonzero effect for at least one trait. Additionally, mvSuSiE provided 95%-level credible sets (**CS**) of putative causal variants, which represent the minimum set of SNPs containing at least one causal SNP with probability of 95% (i.e., the sum of the PIP of these SNPs is equal to or greater than 0.95). To assess the significance of identified CS for traits, mvSuSiE computed the average local false sign rate (***lfsr***; Stephens, 2017), defined as a weighted average of the conditional *lfsr* for all SNPs in the CS. In this study, a CS was considered significant for a trait if the average *lfsr* for that trait was less than 0.05.

Mendelian Randomization Leveraging GWAS and eQTL Data

To identify putative functional genes for body conformation traits, we applied PMR-Egger (Yuan et al., 2020) integrating the ST-GWAS summary data in the "Genome-Wide Association Studies" section and the *cis*-eQTL summary data obtained from the CattleGTEx dataset (Liu et al., 2022). We only selected *cis*-eQTL of blood for our analysis rather than those from other tissues for 2 reasons: (1) blood has the larger sample size (~700), and (2) blood, as part of the systemic circulatory system, plays a crucial role in transporting nutrients to

various organs and tissues (Alexy et al., 2022), which makes blood a general tissue for studying gene expression in relation to body conformation traits. The *P*-values for the MR analysis were adjusted for multiple testing by the false discovery rate control using 0.05 as the significance threshold.

RESULTS

Imputation Accuracies for Different SNP Chips

The imputation accuracies (r^2) for the 3 chips for chromosome 25 are illustrated in Figure 1. The average r^2 values were 0.76 for the 50K chip, 0.82 for the 100K chip, and 0.85 for the 150K chip. After removing the SNPs with MAF <0.05, the average accuracy r^2 was 0.82 for the 50K chip and over 0.9 for the 100K and 150K chips. After filtering with respect to MAF and HWE for the imputed genotypes, we obtained 10,405,093 SNPs for subsequent analysis.

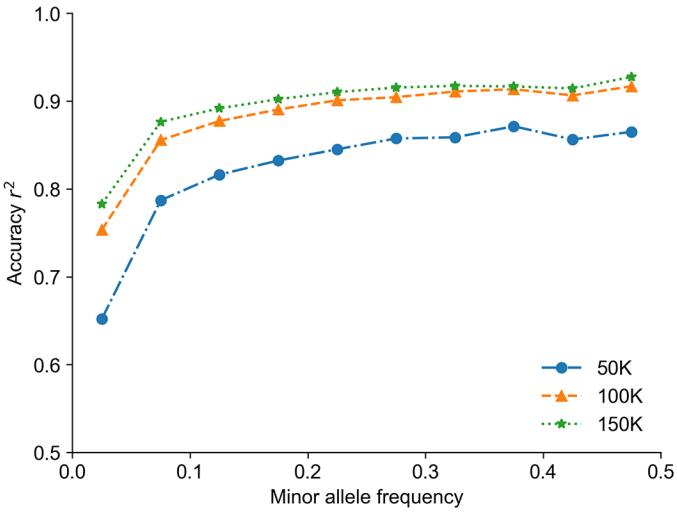

Figure 1. Imputation accuracies (r^2) of different chips (50K, 100K and 150K) for chromosome 25.

Heritability and Genetic Correlation Estimation

The estimates of heritabilities and genetic correlations for the 20 traits are illustrated in Figure 2. The estimated heritabilities of all traits (Figure 2a) were less than 0.15, except these of BH ($\hat{h}^2$ = 0.2177) and PS ($\hat{h}^2$ = 0.1564). The estimated genetic correlations (Figure 2b) ranged from strong negative ($\hat{r}_g$ = −0.5611 for BD-UD) to strong positive ($\hat{r}_g$ = 0.7615 for BQ-FTP). Most trait pairs exhibited low genetic correlation, such as BH-BD ($\hat{r}_g$ = −0.0764), PS-TW ($\hat{r}_g$ = 0.0627), RLSV-RLRV ($\hat{r}_g$ = −0.1430) and RAH-RTP ($\hat{r}_g$ = −0.1081.

ST/MT-GWAS and QTL Regions

The summary results of ST- and MT-GWAS conducted using imputed WGS data are illustrated in Figure 3. At a genome-wide significance level of 1.2×10^{-7} (0.05/422,334), significant association signals of ST-GWAS were identified for only 9 traits (Figure 3a) belonging to 3 trait groups: body, feet and legs, and mammary system (i.e., BH in the body group, FAN, HD, and RLSV in feet and legs group, and UD, FAC, TL, RAW, and RTP in the mammary system group). A total of 22 ST-QTL regions were identified (Supplemental Table S2, see Notes). However, many regions contained only 1 or a few significant SNPs. The sizes of these QTL regions ranged from 1 bp to 159.12 kb with a mean of 30.96 kb, and 82% of them were less than 100 kb. For MT-GWAS (Figure 3b), significant signals were observed in the same 3 trait groups. In total, 12 MT-QTL regions were identified (Supplemental Table S3, see Notes), including one region for the body group, 7 for the feet and legs group, and 4 for the mammary system group. Notably, 7 regions identified by MT-GWAS were overlapped with those by ST-GWAS.

Multitrait Fine-Mapping for Causal Variants

Based on the QTL regions identified by ST- and MT-GWAS, we obtained 25 fine-mapping regions. We then used mvSuSiE to further identify causal variants across traits in 3 trait groups (body, feet and legs, and mammary system) within each fine-mapping region. A total of 30 independent causal signals (95%-level CS) were identified across all fine-mapping regions, with the number of CS per region ranging from 0 to 3 (Figure 4a). Within each CS, the number of SNPs varied from 1 to 372 with a median of 13, and ~27% contained just one SNP (Figure 4b). After filtering based on average *lfsr* <0.05, all CS were significantly associated with one trait, and ~33% of them were associated with 2 or more traits (Figure 4c).

In some fine-mapping regions, the ST-GWAS identified significant associations with only one trait, whereas the multitrait fine-mapping revealed CS which were significantly associated with multiple traits (Supplemental Table S4, see Notes). For example, in the region Chr5:103,068,119–103,580,750, the ST-GWAS only revealed significant associations with BH, whereas no significant associations were observed in the MT-GWAS for the body group (Figure 4d). In contrast, multitrait fine-mapping for all traits in the body group identified 2 independent CS: CS1 and CS2 (Figure 4e). We found that CS1 contained 2 causal SNPs, with the lead SNP (SNP with the largest PIP), 5_103387251, located within the *C1R* gene, had significant effects on 3 body traits

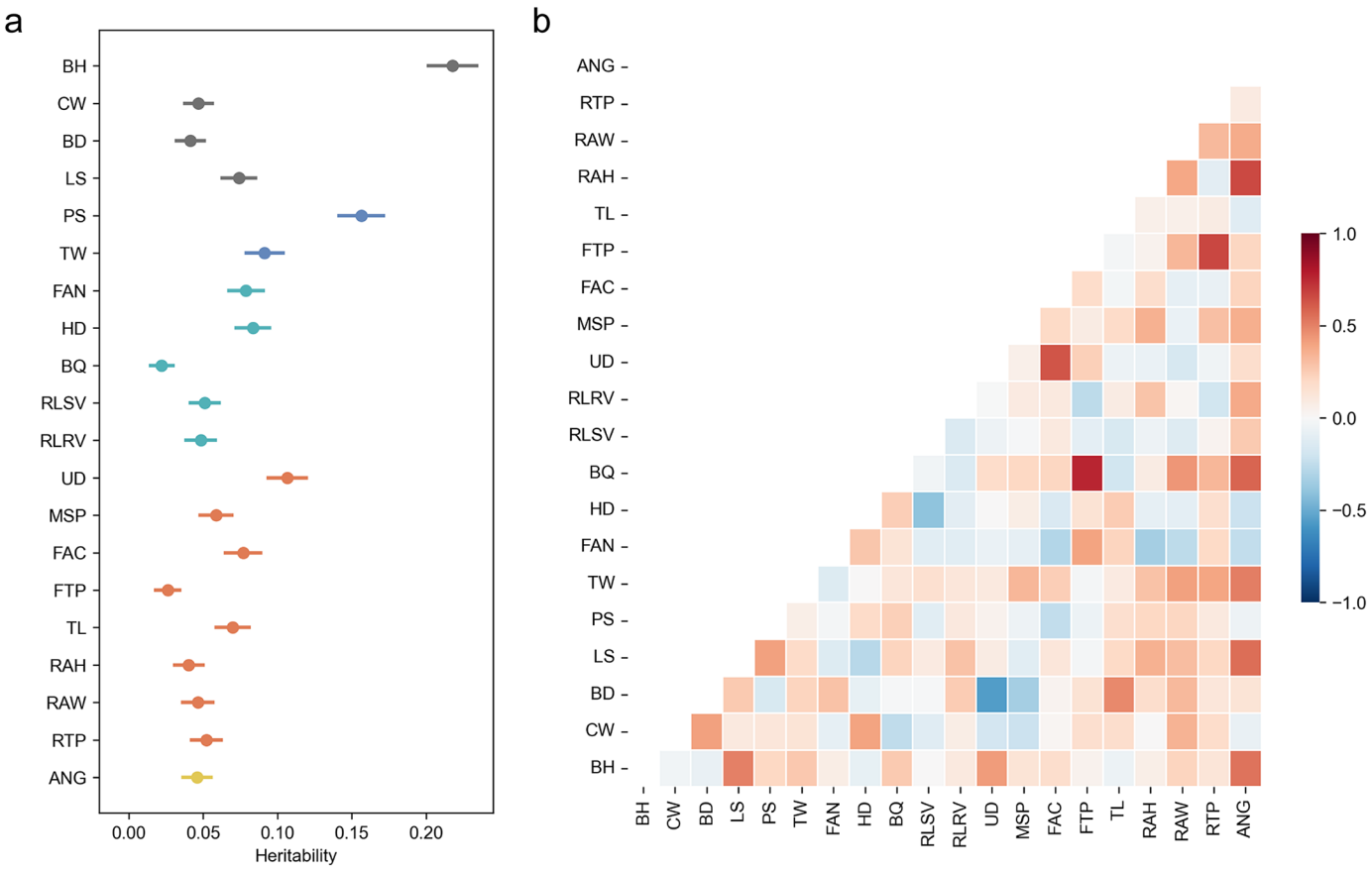

Figure 2. Estimates of heritabilities and genetic correlations for body conformation traits. (a) Estimated heritabilities of all traits. The error bars indicate the SE of the estimates. (b) Estimated genetic correlations across pairs.

(BH, BD, and LS). Similarly, in the region Chr9:11,041,450–11,548,270, significant associations were observed only for HD by ST-GWAS and MT-GWAS identified significant associations with the feet and legs group (Figure 4f), whereas the multitrait fine-mapping revealed a CS which contained only one SNP (9_11294200), located within the *RIMS1* gene, with significant effects on 2 feet and legs traits (FAN and HD; Figure 4g).

Mendelian Randomization for Causal Genes

The results of MR, leveraging ST-GWAS summary data from this study and blood *cis*-eQTL summary data from CattleGTEx (Liu et al., 2022), are illustrated in Figure 5 and Supplemental Figures S1–S4 (see Notes). In total, 153 genes were identified exhibiting significant causal effects on the conformation traits (Supplemental Table S4, see Notes), including 21 on BH, 35 on CW, and 16 on BD. Many genes were found to be associated with multiple traits. For instance, *NETO2* showed significant causal effects on up to 16 traits, and *TTYH3*, *TTC3*, *ANAPC4*, and *PSMD13* exhibited significant causal effects on more than 10 traits. Notably, only one gene, *SERPINB8*, was found to overlap with genes identified through multitrait fine-mapping, with both associated with RAW.

DISCUSSION

Previous GWAS have identified a large number of significant SNPs associated with body conformation traits and concentrated on genes related to significant SNPs or top SNPs within QTL regions (Nazar et al., 2022; Haque et al., 2023; Li et al., 2024). However, the top SNPs within QTL regions are rarely causal variants (van de Bunt et al., 2015). In this study, we performed ST- and MT-GWAS on body conformation traits using sequence-level genotype data in a Chinese Holstein population and further employed multitrait fine-mapping to identify causal variants. Furthermore, we applied MR analysis to integrate ST-GWAS and *cis*-eQTL data, aiming to identify putative functional genes underlying these traits.

We estimated heritabilities and genetic correlations across body conformation traits. The heritability estimates of body conformation traits in this study are lower

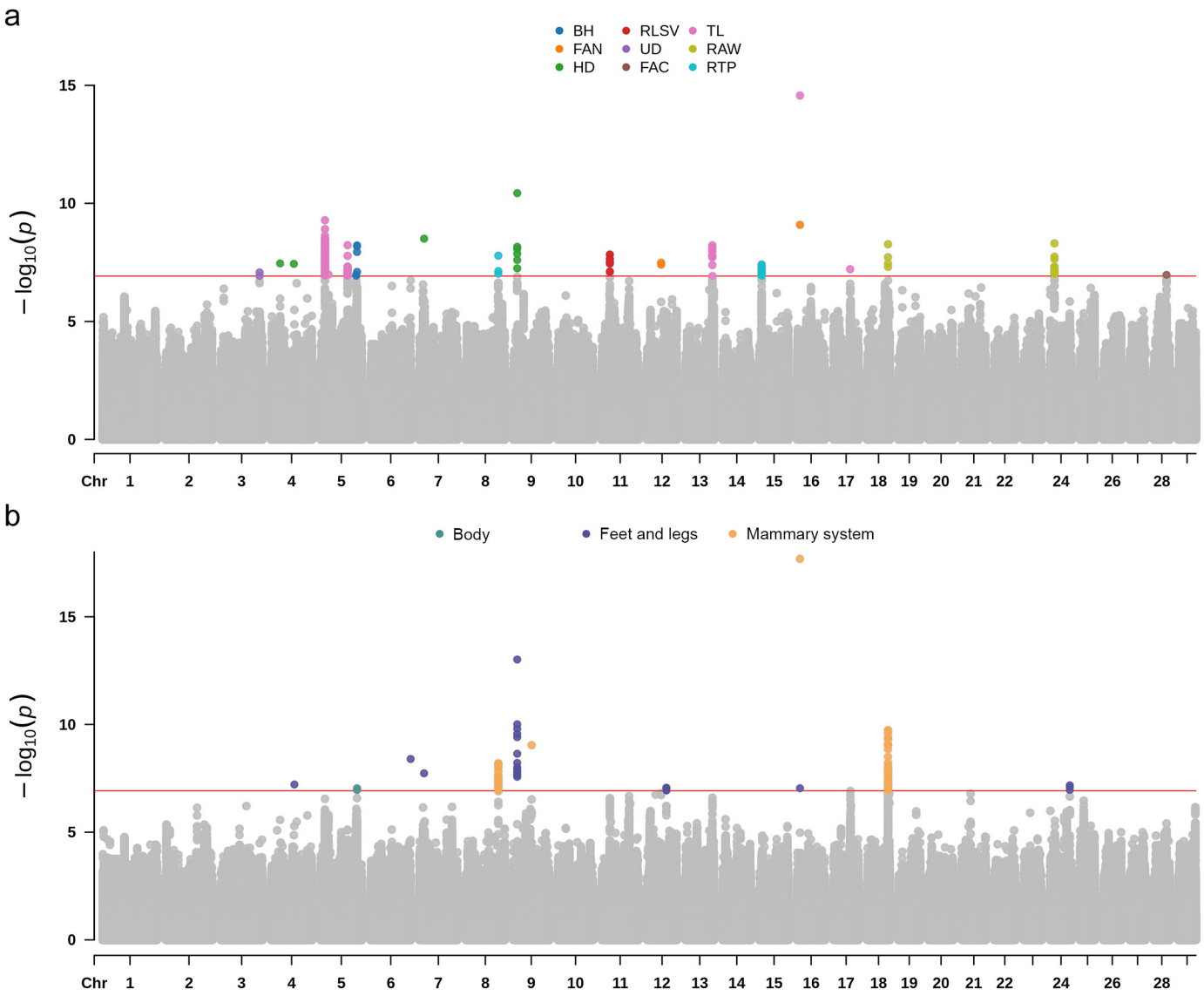

Figure 3. Summary Manhattan plot of (a) single-trait and (b) multitrait GWAS for body conformation traits. The red lines indicate the significance threshold ($P = 1.2 \times 10^{-7}$). Chr = chromosome.

than those reported in most previous studies in Holstein cattle, such as those in German Holstein cattle (Schmidtmann et al., 2023) and Nordic Holstein cattle (Mehtiö et al., 2021). However, our estimates are consistent with previous studies in Chinese Holstein cattle (Wu et al., 2013; Olasege et al., 2019). Furthermore, the heritability estimates in other breeds, such as Italian Jersey cattle (Roveglia et al., 2019), agree with our estimates. Heritabilities and their estimates are population-specific and could vary due to factors such as the scale used for scoring, genetic background, population structure, environmental variations, and statistical model. The estimated genetic correlations for most trait pairs were weak. This is consistent with the results of most other studies. For example, the genetic correlation between PS and PW ($\hat{r}_g$ = 0.0627) was close to that obtained by Oliveira Junior et al. (2021; $\hat{r}_g$ = 0.07). However, some trait pairs also exhibited strong positive or negative genetic correlations. For instance, FTP and RTP in the mammary system group exhibited strong positive genetic correlation ($\hat{r}_g$ = 0.6712), which agreed with previous studies (Oliveira Junior et al., 2021; Xue et al., 2022). It should be noted that the genetic correlations for trait pairs within groups were stronger than those between groups.

Considering the relative genetic correlations between traits within trait groups, we performed multitrait fine-mapping for traits within groups to improve the ability

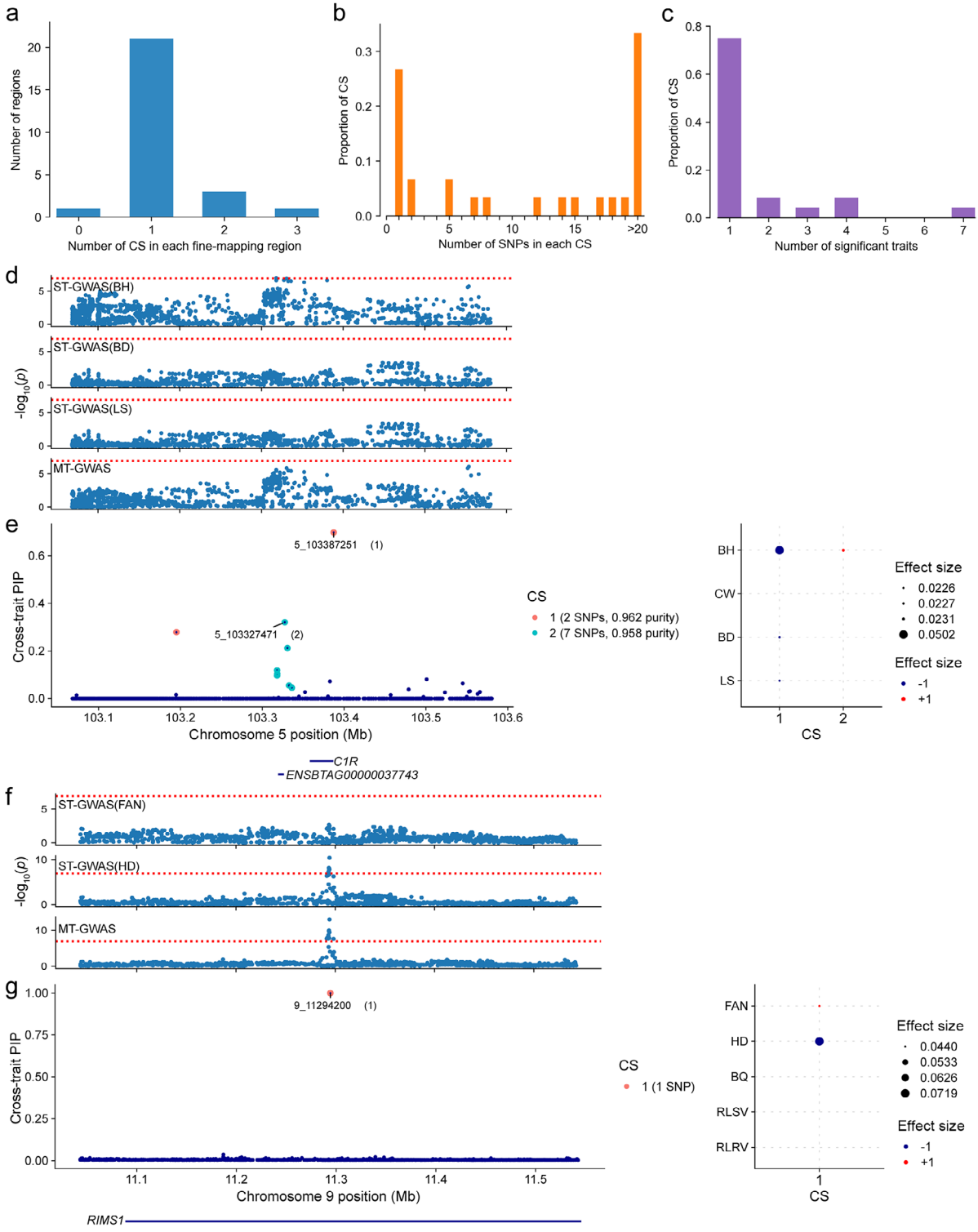

Figure 4. Summary of multitrait fine-mapping results. (a) Number of credible sets (CS) of causal SNPs identified in each fine-mapping region. (b) Number of significant SNPs in each CS. (c) Number of significantly associated traits (average *lfsr* < 0.05) in each CS. Local Manhattan plot of GWAS-results in the region Chr5:103,068,119–103,580,750 (d) and Chr9:11,041,450–11,548,270 (f). The dotted red line indicates the significance threshold ($P = 1.2 \times 10^{-7}$). The results of multitrait fine-mapping in the region Chr5:103,068,119–103,580,750 (e) and Chr9:11,041,450–11,548,270 (g). The left-hand part shows the cross-trait posterior inclusion probabilities (PIP) for each SNP in the QTL region. The labeled SNPs are the "lead SNPs" (i.e., SNPs with the highest cross-trait PIP in each CS). "Purity" is defined as the minimum absolute pairwise correlation (Pearson's r) among SNPs in the CS. The related genes of the lead SNPs are displayed below. The right-hand part shows the posterior effect estimates of the sentinel SNPs whenever the CS is significant for the given trait (average *lfsr* < 0.05).

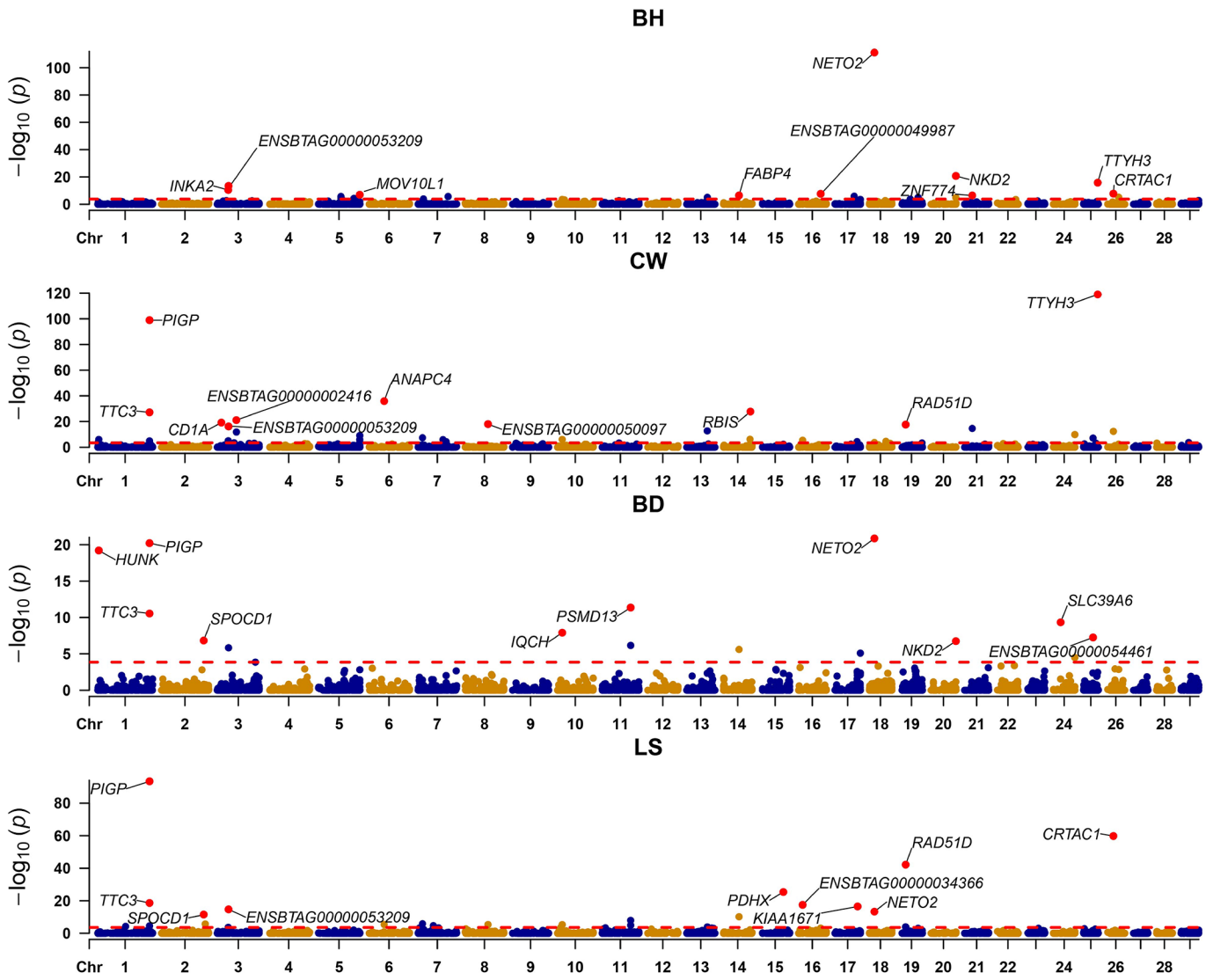

Figure 5. Manhattan plot of results for Mendelian randomization analysis in the body trait group. The red straight line indicates the significance threshold of the false discovery rate = 0.05. The genes labeled in the plot correspond to the top 10 most significant associations. Chr = chromosome.

for identifying causal SNPs in the fine-mapping regions from ST- and MT-GWAS. We identified 30 independent CS with significant causal effects on at least one trait. Among these, CS1 within the region Chr5:103,068,119–103,580,750 was significant for BH, BD, and LS. We found 2 SNPs in this CS, and the lead SNP (5_103387251, PIP = 0.6977) is a missense variant (p.Glu702Lys) in the *C1R* gene. *C1R*, a member of the peptidase S1 protein family, is the first component of the classical pathway of the complement system. The regulation and magnitude of complement responses can influence skeletal muscle aging-related (Graca et al., 2023), muscle fibrosis (Hajishengallis et al., 2017), and muscle mass and strength (Naito et al., 2012). To explore the potential mechanisms underlying the effects of this missense variant, we used DynaMut2 (Rodrigues et al., 2021) to predict the protein stability changes upon to this missense mutation. The predicted stability change between the wild and mutant-type proteins was −0.08 kcal/mol, which can be classified as "destabilizing." Notably, 8 CS contained only one SNP, suggesting they are high-confidence candidate causal SNPs. For example, CS1 in the region Chr9:11,041,450–11,548,270 contained only one SNP (9_11294200, PIP = 1) with significant effects on FAN and HD. This SNP is located in an intron of the *RIMS1* gene. In humans, polyostotic fibrous dysplasia, a bone disease, may be related to mutations in *RIMS1* (Lin et al., 2020). In addition, *RIMS1* may play a role in neuromuscular junction development, in which dysfunction causes motor disorders and muscle wasting (Hui

et al., 2021). Interestingly, both *C1R* and *RIMS1* were also found significantly associated with fat percentage in US Holstein cattle (Jiang et al., 2019b). Additionally, several genes identified through fine-mapping have been reported in previous GWAS, such as *CCND2* associated with BH (Abo-Ismail et al., 2017), *TMTC2* associated with TL (Abo-Ismail et al., 2017), and *NRG3* associated with UD (Cole et al., 2011).

Furthermore, as a complement to conventional GWAS, MR integrates GWAS and eQTL data to identify putative causal genes. In our MR analysis, leveraging ST-GWAS summary data from this study and blood *cis*-eQTL summary data from CattleGTEx, we identified several putative causal genes associated with various body conformation traits. Notably, only one gene, *SERPINB8*, was found to overlap with the genes identified through multitrait fine-mapping. The *SERPINB8* gene was associated with RAW in both the fine-mapping and MR analysis. However, there were no previous reports about the association of *SERPINB8* with RAW in cattle. In addition, other genes, including *NETO2*, *TTYH3*, *TTC3*, *ANAPC4*, and *PSMD13*, demonstrated significant causal effects with more than 10 traits. *NETO2* encodes a transmembrane protein that is essential for proper neurological function (Fedorova et al., 2017). The *TTYH3* gene is highly expressed in excitatory tissues such as skeletal muscle, where it regulates cell volume and signal transduction (Biswas et al., 2022). *TTC3*, an E3 ubiquitin ligase, plays a role in myofibroblast differentiation (Kim et al., 2019), and has been previously reported to be associated with milk yield, fat percentage, and protein percentage in US Holstein cattle (Jiang et al., 2019b). *ANAPC4*, also an E3 ubiquitin ligase, regulates mitosis and the G1 phase, thereby influencing the cell cycle (Liu et al., 2023), and has been identified as a candidate gene for carcass weight in Korean Hanwoo cattle (Bhuiyan et al., 2018). *PSMD13* was recognized as a myostatin-dependent gene in Holstein-Friesian bulls (Sadkowski et al., 2008).

CONCLUSIONS

In summary, we conducted ST- and MT-GWAS for body conformation traits in Chinese Holstein cattle, followed by multitrait fine-mapping and MR to reveal causal variants and genes. A total of 27 QTL regions associated with body conformation traits were identified. Subsequent fine-mapping and MR analysis revealed several putative causal genes, including a few previously reported genes (*CCND2*, *TMTC2*, and *NRG3*) and several novel identified genes (*C1R*, *RIMS1*, *SERPINB8*, *NETO2*, *TTYH3*, *TTC3*, *ANAPC4*, and *PSMD13*). These findings enhanced our understanding of the genetic architecture underlying body conformation traits in cattle.

NOTES

This work was supported by the National Key Research and Development Program of China (2021YFD1200903, 2023ZD0404901, and 2021YFF1000701; Beijing, China), Taishan Scholar Foundation of Shandong Province (tsqnz20231240; Shandong, China), Shandong Provincial Natural Science Foundation (ZR2023QC252 and ZR2021MC070; Shandong, China), Shandong Cattle Research System (SDAIT-09-02; Shandong, China), Key R&D Program of Shandong Province (2023LZGC004; Shandong, China), the Earmarked Fund for CARS-36 (Beijing, China), and the Project of Genetic Improvement for Agricultural Species of Shandong Province (2019LZGC011; Shandong, China). Supplemental material for this article is available at https://doi.org/10.6084/m9.figshare.28558289. The guidelines of experimental animal management of Shandong Agricultural University (SDAU) were followed throughout the study, and the experimental protocols were approved by the Experimental Animal Care and Use Committee of SDAU. The authors have not stated any conflicts of interest.

Nonstandard abbreviations used: ANG = angularity; BD = body depth; BH = body height; BQ = bone quality; Chr = chromosome; CS = credible set; CW = chest width; eQTL = expression QTL; FAC = for attachment; FAN = foot angle; FTP = for teat placement; HD = heel depth; HWE = Hardy–Weinberg equilibrium; LD = linkage disequilibrium; *lfsr* = local false sign rate; LS = loin strength; MAF = minor allele frequency; MR = Mendelian randomization; MSP = median suspensory; MT = multitrait; PIP = posterior inclusion probability; PMR-Egger = probabilistic MR-Egger; PS = pin setting; RAH = rear attach height; RAW = rear attach width; RLRV = rear legs rear view; RLSV = rear legs side view; RTP = rear teat placement; ST = single-trait; TL = teat length; TW = thurl width; UD = udder depth; WGS = whole-genome sequence.

REFERENCES

Abo-Ismail, M. K., L. F. Brito, S. P. Miller, M. Sargolzaei, D. A. Grossi, S. S. Moore, G. Plastow, P. Stothard, S. Nayeri, and F. S. Schenkel. 2017. Genome-wide association studies and genomic prediction of breeding values for calving performance and body conformation traits in Holstein cattle. Genet. Sel. Evol. 49:82. https://doi.org/10.1186/s12711-017-0356-8.

Alexy, T., J. Detterich, P. Connes, K. Toth, E. Nader, P. Kenyeres, J. Arriola-Montenegro, P. Ulker, and M. J. Simmonds. 2022. Physical properties of blood and their relationship to clinical conditions. Front. Physiol. 13:906768. https://doi.org/10.3389/fphys.2022.906768.

Benner, C., C. C. Spencer, A. S. Havulinna, V. Salomaa, S. Ripatti, and M. Pirinen. 2016. FINEMAP: Efficient variable selection using summary data from genome-wide association studies. Bioinformatics 32:1493–1501. https://doi.org/10.1093/bioinformatics/btw018.

Bhuiyan, M. S. A., D. Lim, M. Park, S. Lee, Y. Kim, C. Gondro, B. Park, and S. Lee. 2018. Functional Partitioning of genomic variance and genome-wide association study for carcass traits in Korean Hanwoo cattle using imputed sequence level SNP data. Front. Genet. 9:217. https://doi.org/10.3389/fgene.2018.00217.

Biswas, P. K., Y. Kwak, A. Kim, J. Seok, H. J. Kwak, M. Lee, A. A. Dayem, K. Song, J. Y. Park, K. S. Park, H. J. Shin, and S. G. Cho. 2022. TTYH3 modulates bladder cancer proliferation and metastasis via FGFR1/H-Ras/A-Raf/MEK/ERK pathway. Int. J. Mol. Sci. 23:10496. https://doi.org/10.3390/ijms231810496.

Bowden, J., G. Davey Smith, and S. Burgess. 2015. Mendelian randomization with invalid instruments: effect estimation and bias detection through Egger regression. Int. J. Epidemiol. 44:512–525. https://doi.org/10.1093/ije/dyv080.

Browning, B. L., Y. Zhou, and S. R. Browning. 2018. A One-penny imputed genome from next-generation reference panels. Am. J. Hum. Genet. 103:338–348. https://doi.org/10.1016/j.ajhg.2018.07.015.

Chepelev, I., I. Harley, and J. B. Harley. 2023. Modeling of horizontal pleiotropy identifies possible causal gene expression in systemic lupus erythematosus. Front Lupus 1:1234578. https://doi.org/10.3389/flupu.2023.1234578.

Cole, J. B., G. R. Wiggans, L. Ma, T. S. Sonstegard, T. J. Lawlor Jr., B. A. Crooker, C. P. Van Tassell, J. Yang, S. Wang, L. K. Matukumalli, and Y. Da. 2011. Genome-wide association analysis of thirty one production, health, reproduction and body conformation traits in contemporary U.S. Holstein cows. BMC Genomics 12:408. https://doi.org/10.1186/1471-2164-12-408.

Fedorova, M. S., A. V. Snezhkina, E. A. Pudova, I. S. Abramov, A. V. Lipatova, S. L. Kharitonov, A. F. Sadritdinova, K. M. Nyushko, K. M. Klimina, M. M. Belyakov, E. N. Slavnova, N. V. Melnikova, M. A. Chernichenko, D. V. Sidorov, M. V. Kiseleva, A. D. Kaprin, B. Y. Alekseev, A. A. Dmitriev, and A. V. Kudryavtseva. 2017. Upregulation of NETO2 gene in colorectal cancer. BMC Genet. 18(Suppl. 1):117. https://doi.org/10.1186/s12863-017-0581-8.

Graca, F. A., B. A. Minden-Birkenmaier, A. Stephan, F. Demontis, and M. Labelle. 2023. Signaling roles of platelets in skeletal muscle regeneration. BioEssays 45:2300134. https://doi.org/10.1002/bies.202300134.

Gusev, A., A. Ko, H. Shi, G. Bhatia, W. Chung, B. W. Penninx, R. Jansen, E. J. de Geus, D. I. Boomsma, F. A. Wright, P. F. Sullivan, E. Nikkola, M. Alvarez, M. Civelek, A. J. Lusis, T. Lehtimaki, E. Raitoharju, M. Kahonen, I. Seppala, O. T. Raitakari, J. Kuusisto, M. Laakso, A. L. Price, P. Pajukanta, and B. Pasaniuc. 2016. Integrative approaches for large-scale transcriptome-wide association studies. Nat. Genet. 48:245–252. https://doi.org/10.1038/ng.3506.

Hajishengallis, G., E. S. Reis, D. C. Mastellos, D. Ricklin, and J. D. Lambris. 2017. Novel mechanisms and functions of complement. Nat. Immunol. 18:1288–1298. https://doi.org/10.1038/ni.3858.

Haque, M. A., M. Z. Alam, A. Iqbal, Y. M. Lee, C. G. Dang, and J. J. Kim. 2023. Genome-wide association studies for body conformation traits in Korean Holstein population. Animals (Basel) 13:2964. https://doi.org/10.3390/ani13182964.

Hayes, B. J., and H. D. Daetwyler. 2019. 1000 Bull Genomes Project to map simple and complex genetic traits in cattle: Applications and outcomes. Annu. Rev. Anim. Biosci. 7:89–102. https://doi.org/10.1146/annurev-animal-020518-115024.

Hemerich, D., V. Svenstrup, V. D. Obrero, M. Preuss, A. Moscati, J. N. Hirschhorn, and R. Loos. 2024. An integrative framework to prioritize genes in more than 500 loci associated with body mass index. Am. J. Hum. Genet. 111:1035–1046. https://doi.org/10.1016/j.ajhg.2024.04.016.

Hui, T., H. Jing, and X. Lai. 2021. Neuromuscular junction-specific genes screening by deep RNA-seq analysis. Cell Biosci. 11:81. https://doi.org/10.1186/s13578-021-00590-9.

Jiang, J., J. B. Cole, E. Freebern, Y. Da, P. M. VanRaden, and L. Ma. 2019a. Functional annotation and Bayesian fine-mapping reveals candidate genes for important agronomic traits in Holstein bulls. Commun. Biol. 2:212. https://doi.org/10.1038/s42003-019-0454-y.

Jiang, J., L. Ma, D. Prakapenka, P. M. VanRaden, J. B. Cole, and Y. Da. 2019b. A Large-scale genome-wide association study in U.S. Holstein cattle. Front. Genet. 10:412. https://doi.org/10.3389/fgene.2019.00412.

Jiang, Y., Y. Zhang, C. Ju, R. Zhang, H. Li, F. Chen, Y. Zhu, S. Shen, and Y. Wei. 2023. A cross-disorder study to identify causal relationships, shared genetic variants, and genes across 21 digestive disorders. iScience 26:108238. https://doi.org/10.1016/j.isci.2023.108238.

Kim, E. S., and B. W. Kirkpatrick. 2009. Linkage disequilibrium in the North American Holstein population. Anim. Genet. 40:279–288. https://doi.org/10.1111/j.1365-2052.2008.01831.x.

Kim, J. H., S. Ham, Y. Lee, G. Y. Suh, and Y. S. Lee. 2019. TTC3 contributes to TGF-β_1-induced epithelial-mesenchymal transition and myofibroblast differentiation, potentially through SMURF2 ubiquitylation and degradation. Cell Death Dis. 10:92. https://doi.org/10.1038/s41419-019-1308-8.

Köck, A., M. Ledinek, L. Gruber, F. Steininger, B. Fuerst-Waltl, and C. Egger-Danner. 2018. Genetic analysis of efficiency traits in Austrian dairy cattle and their relationships with body condition score and lameness. J. Dairy Sci. 101:445–455. https://doi.org/10.3168/jds.2017-13281.

Li, S., F. Ge, L. Chen, Y. Liu, Y. Chen, and Y. Ma. 2024. Genome-wide association analysis of body conformation traits in Chinese Holstein Cattle. BMC Genomics 25:1174. https://doi.org/10.1186/s12864-024-11090-8.

Lin, T., X. Y. Li, C. Y. Zou, W. W. Liu, J. F. Lin, X. X. Zhang, S. Q. Zhao, X. B. Xie, G. Huang, J. Q. Yin, and J. N. Shen. 2020. Discontinuous polyostotic fibrous dysplasia with multiple systemic disorders and unique genetic mutations: A case report. World J. Clin. Cases 8:6197–6205. https://doi.org/10.12998/wjcc.v8.i23.6197.

Liu, S., Y. Gao, O. Canela-Xandri, S. Wang, Y. Yu, W. Cai, B. Li, R. Xiang, A. J. Chamberlain, E. Pairo-Castineira, K. D'Mellow, K. Rawlik, C. Xia, Y. Yao, P. Navarro, D. Rocha, X. Li, Z. Yan, C. Li, B. D. Rosen, C. P. Van Tassell, P. M. Vanraden, S. Zhang, L. Ma, J. B. Cole, G. E. Liu, A. Tenesa, and L. Fang. 2022. A multi-tissue atlas of regulatory variants in cattle. Nat. Genet. 54:1438–1447. https://doi.org/10.1038/s41588-022-01153-5.

Liu, W., Y. Wang, L. Bozi, P. D. Fischer, M. P. Jedrychowski, H. Xiao, T. Wu, N. Darabedian, X. He, E. L. Mills, N. Burger, S. Shin, A. Reddy, H. G. Sprenger, N. Tran, S. Winther, S. M. Hinshaw, J. Shen, H. S. Seo, K. Song, A. Z. Xu, L. Sebastian, J. J. Zhao, S. Dhe-Paganon, J. Che, S. P. Gygi, H. Arthanari, and E. T. Chouchani. 2023. Lactate regulates cell cycle by remodelling the anaphase promoting complex. Nature 616:790–797. https://doi.org/10.1038/s41586-023-05939-3.

Mai, J., M. Lu, Q. Gao, J. Zeng, and J. Xiao. 2023. Transcriptome-wide association studies: recent advances in methods, applications and available databases. Commun. Biol. 6:899. https://doi.org/10.1038/s42003-023-05279-y.

Mehtiö, T., T. Pitkanen, A. M. Leino, E. A. Mantysaari, R. Kempe, E. Negussie, and M. H. Lidauer. 2021. Genetic analyses of metabolic body weight, carcass weight and body conformation traits in Nordic dairy cattle. Animal 15:100398. https://doi.org/10.1016/j.animal.2021.100398.

Naito, A. T., T. Sumida, S. Nomura, M. L. Liu, T. Higo, A. Nakagawa, K. Okada, T. Sakai, A. Hashimoto, Y. Hara, I. Shimizu, W. Zhu, H. Toko, A. Katada, H. Akazawa, T. Oka, J. K. Lee, T. Minamino, T. Nagai, K. Walsh, A. Kikuchi, M. Matsumoto, M. Botto, I. Shiojima, and I. Komuro. 2012. Complement C1q activates canonical Wnt signaling and promotes aging-related phenotypes. Cell 149:1298–1313. https://doi.org/10.1016/j.cell.2012.07.014.

Nazar, M., I. M. Abdalla, Z. Chen, N. Ullah, Y. Liang, S. Chu, T. Xu, Y. Mao, Z. Yang, and X. Lu. 2022. Genome-wide association study for udder conformation traits in Chinese Holstein cattle. Animals (Basel) 12:2542. https://doi.org/10.3390/ani12192542.

Ning, C., D. Wang, H. Kang, R. Mrode, L. Zhou, S. Xu, and J. F. Liu. 2018. A rapid epistatic mixed-model association analysis by linear retransformations of genomic estimated values. Bioinformatics 34:1817–1825. https://doi.org/10.1093/bioinformatics/bty017.

Olasege, B. S., S. Zhang, Q. Zhao, D. Liu, H. Sun, Q. Wang, P. Ma, and Y. Pan. 2019. Genetic parameter estimates for body conformation traits using composite index, principal component, and factor

analysis. J. Dairy Sci. 102:5219–5229. https://doi.org/10.3168/jds.2018-15561.
Oliveira Junior, J. G., F. S. Schenkel, L. Alcantara, K. Houlahan, C. Lynch, and C. F. Baes. 2021. Estimated genetic parameters for all genetically evaluated traits in Canadian Holsteins. J. Dairy Sci. 104:9002–9015. https://doi.org/10.3168/jds.2021-20227.
Pedrosa, V. B., F. S. Schenkel, S. Y. Chen, H. R. Oliveira, T. M. Casey, M. G. Melka, and L. F. Brito. 2021. Genomewide association analyses of lactation persistency and milk production traits in Holstein cattle based on imputed whole-genome sequence data. Genes (Basel) 12:1830. https://doi.org/10.3390/genes12111830.
Purcell, S., B. Neale, K. Todd-Brown, L. Thomas, M. A. Ferreira, D. Bender, J. Maller, P. Sklar, P. I. de Bakker, M. J. Daly, and P. C. Sham. 2007. PLINK: A tool set for whole-genome association and population-based linkage analyses. Am. J. Hum. Genet. 81:559–575. https://doi.org/10.1086/519795.
Qi, T., L. Song, Y. Guo, C. Chen, and J. Yang. 2024. From genetic associations to genes: methods, applications, and challenges. Trends Genet. 40:642–667. https://doi.org/10.1016/j.tig.2024.04.008.
Rodrigues, C. H. M., D. E. V. Pires, and D. B. Ascher. 2021. DynaMut2: Assessing changes in stability and flexibility upon single and multiple point missense mutations. Protein Sci. 30:60–69. https://doi.org/10.1002/pro.3942.
Roveglia, C., G. Niero, T. Bobbo, M. Penasa, R. Finocchiaro, G. Visentin, N. Lopez-Villalobos, and M. Cassandro. 2019. Genetic parameters for linear type traits including locomotion in Italian Jersey cattle breed. Livest. Sci. 229:131–136. https://doi.org/10.1016/j.livsci.2019.09.023.
Sadkowski, T., M. Jank, L. Zwierzchowski, E. Siadkowska, J. Oprzadek, and T. Motyl. 2008. Gene expression profiling in skeletal muscle of Holstein-Friesian bulls with single-nucleotide polymorphism in the myostatin gene 5′-flanking region. J. Appl. Genet. 49:237–250. https://doi.org/10.1007/BF03195620.
Schmidtmann, C., D. Segelke, J. Bennewitz, J. Tetens, and G. Thaller. 2023. Genetic analysis of production traits and body size measurements and their relationships with metabolic diseases in German Holstein cattle. J. Dairy Sci. 106:421–438. https://doi.org/10.3168/jds.2022-22363.
Servin, B., and M. Stephens. 2007. Imputation-based analysis of association studies: Candidate regions and quantitative traits. PLoS Genet. 3:e114. https://doi.org/10.1371/journal.pgen.0030114.
Singh, S., A. Choudhury, S. Hazelhurst, N. J. Crowther, P. R. Boua, H. Sorgho, G. Agongo, E. A. Nonterah, L. K. Micklesfield, S. A. Norris, I. Kisiangani, S. Mohamed, F. X. Gomez-Olive, S. M. Tollman, S. Choma, J. T. Brandenburg, and M. Ramsay. 2023. Genome-wide association study meta-analysis of blood pressure traits and hypertension in sub-Saharan African populations: An AWI-Gen study. Nat. Commun. 14:8376. https://doi.org/10.1038/s41467-023-44079-0.
Stephens, M. 2017. False discovery rates: A new deal. Biostatistics 18:275–294. https://doi.org/10.1093/biostatistics/kxw041.
Teng, J., D. Wang, C. Zhao, X. Zhang, Z. Chen, J. Liu, D. Sun, H. Tang, W. Wang, J. Li, C. Mei, Z. Yang, C. Ning, and Q. Zhang. 2023. Longitudinal genome-wide association studies of milk production traits in Holstein cattle using whole-genome sequence data imputed from medium-density chip data. J. Dairy Sci. 106:2535–2550. https://doi.org/10.3168/jds.2022-22277.
Uffelmann, E., Q. Q. Huang, N. S. Munung, J. de Vries, Y. Okada, A. R. Martin, H. C. Martin, T. Lappalainen, and D. Posthuma. 2021. Genome-wide association studies. Nat. Rev. Methods Primers 1:59. https://doi.org/10.1038/s43586-021-00056-9.
van de Bunt, M., A. Cortes, M. A. Brown, A. P. Morris, and M. I. McCarthy. 2015. Evaluating the performance of fine-mapping strategies at common variant GWAS loci. PLoS Genet. 11:e1005535. https://doi.org/10.1371/journal.pgen.1005535.
VanRaden, P. M. 2008. Efficient methods to compute genomic predictions. J. Dairy Sci. 91:4414–4423. https://doi.org/10.3168/jds.2007-0980.
Wang, G., A. Sarkar, P. Carbonetto, and M. Stephens. 2020. A simple new approach to variable selection in regression, with application to genetic fine mapping. J. R. Stat. Soc. Series B Stat. Methodol. 82:1273–1300. https://doi.org/10.1111/rssb.12388.
Wang, X., J. Yang, J. Xue, M. Zhang, F. Zhang, K. Wang, Y. Li, Y. Zhang, X. Wu, F. Wang, X. Zhao, J. Ni, Y. Ma, R. Li, L. Wang, G. Su, Y. Gao, and J. Li. 2024. Genetic parameters of semen traits and their correlations with conformation traits in Chinese Holstein bulls. Vet. Med. Int. 2024:5593703. https://doi.org/10.1155/2024/5593703.
Wu, X., M. Fang, L. Liu, S. Wang, J. Liu, X. Ding, S. Zhang, Q. Zhang, Y. Zhang, L. Qiao, M. S. Lund, G. Su, and D. Sun. 2013. Genome wide association studies for body conformation traits in the Chinese Holstein cattle population. BMC Genomics 14:897. https://doi.org/10.1186/1471-2164-14-897.
Xue, X., H. Hu, J. Zhang, Y. Ma, L. Han, F. Hao, Y. Jiang, and Y. Ma. 2022. Estimation of genetic parameters for conformation traits and milk production traits in Chinese Holsteins. Animals (Basel) 13:100. https://doi.org/10.3390/ani13010100.
Yang, J., S. H. Lee, M. E. Goddard, and P. M. Visscher. 2011. GCTA: A tool for genome-wide complex trait analysis. Am. J. Hum. Genet. 88:76–82. https://doi.org/10.1016/j.ajhg.2010.11.011.
Yang, Y., H. Musco, S. Simpson-Yap, Z. Zhu, Y. Wang, X. Lin, J. Zhang, B. Taylor, J. Gratten, and Y. Zhou. 2021. Investigating the shared genetic architecture between multiple sclerosis and inflammatory bowel diseases. Nat. Commun. 12:5641. https://doi.org/10.1038/s41467-021-25768-0.
Yuan, Z., H. Zhu, P. Zeng, S. Yang, S. Sun, C. Yang, J. Liu, and X. Zhou. 2020. Testing and controlling for horizontal pleiotropy with probabilistic Mendelian randomization in transcriptome-wide association studies. Nat. Commun. 11:3861. https://doi.org/10.1038/s41467-020-17668-6.
Zhu, Z., F. Zhang, H. Hu, A. Bakshi, M. R. Robinson, J. E. Powell, G. W. Montgomery, M. E. Goddard, N. R. Wray, P. M. Visscher, and J. Yang. 2016. Integration of summary data from GWAS and eQTL studies predicts complex trait gene targets. Nat. Genet. 48:481–487. https://doi.org/10.1038/ng.3538.